Journal of Materials Chemistry C

ROYAL SOCIETY OF CHEMISTRY

REVIEW

View Article Online
View Journal | View Issue

Cite this: J. Mater. Chem. C, 2022, 10, 2375

Recent progress in single-molecule transistors: their designs, mechanisms and applications

Huanyan Fu,†[ab] Xin Zhu,†[ab] Peihui Li,[a] Mengmeng Li,[a] Lan Yang,[a] Chuancheng Jia *[a] and Xuefeng Guo *[ab]

Received 29th August 2021,
Accepted 26th October 2021

DOI: 10.1039/d1tc04079k

rsc.li/materials-c

Single-molecule field-effect transistors (FETs) are the key building blocks of future electronic circuits. At the same time, they are also a unique platform for studying physical mechanisms at the single-molecule level. How to construct single-molecule FETs and how to efficiently control the charge transfer characteristics of the devices are two core issues in the development of single-molecule FETs. In this review, we present the research progress in single-molecule FETs with solid or liquid gates. Strategies to design single-molecule FETs are emphasized, including the design of functional molecules, the construction of gate electrodes and the control of molecule–electrode interface coupling. These single-molecule FETs provide a basis for practical applications and the exploration of physical laws. Specifically, the physical mechanisms of single-molecule FETs, especially those related to interfacial coupling, are explained, such as the energy level shift, Coulomb blockade effect, Kondo effect and electron–phonon coupling. The applications of single-molecule FETs are summarized, including the regulation of quantum interference, spin, thermoelectric effect and superconductivity. Finally, the current opportunities and challenges in the field of single-molecule FETs are proposed, aiming to promote the future development of single-molecule electronics.

1. Introduction

Single-molecule field-effect transistors (FETs) are not only an important part of future integrated circuits, but also an effective experimental platform for studying the physical and chemical laws at the molecular scale.[1–7] The current research of single-molecule transistors mainly focuses on two aspects. One is how to design and construct various types of single-molecule FETs technically, and the other is to use single-molecule FETs as experimental platforms to explore the laws and realize various

[a] Center of Single-Molecule Sciences, Institute of Modern Optics, Tianjin Key Laboratory of Micro-scale Optical Information Science and Technology, Frontiers Science Center for New Organic Matter, College of Electronic Information and Optical Engineering, Nankai University, 38 Tongyan Road, Jinnan District, Tianjin 300350, P. R. China. E-mail: guoxf@pku.edu.cn, jiacc@nankai.edu.cn
[b] State Key Laboratory for Structural Chemistry of Unstable and Stable Species, Beijing National Laboratory for Molecular Sciences, National Biomedical Imaging Center, College of Chemistry and Molecular Engineering, Peking University, Beijing 100871, P. R. China
† H. Y. F. and X. Z. contributed equally to this review.

Huanyan Fu

Huanyan Fu is currently a PhD candidate at the Center of Single-Molecule Science, Institute of Modern Optics, College of Electronic Information and Optical Engineering, Nankai University, with Prof. Xuefeng Guo. Her research is focused on the device physics of single-molecule junctions.

Xin Zhu

Xin Zhu is currently a PhD candidate at the Center of Single-Molecule Science, Institute of Modern Optics, College of Electronic Information and Optical Engineering, Nankai University, with Prof. Xuefeng Guo. Her research is focused on single-molecule dynamics.

specific applications.[8–11] Specifically, the design of single-molecule FETs needs to consider the following aspects. First is the design of the gate, including the gate type, the selection of the dielectric layer material and the relative position between the gate and source/drain electrodes.[12–14] The second is molecular characteristics, mainly to design the molecular structure.[15–18] The third is the molecule–electrode interface, especially the interface connection and electronic coupling between the molecule and electrode.[19–21] With novel designs, a series of breakthroughs in single-molecule FETs have been achieved, especially in the exploration of scientific laws and specific applications.

Single-molecule FETs work based on quantum mechanics. The role of the gate is not only to simply realize the function of switching, but also to modulate the molecular orbitals and change the electronic and spin states of the molecule.[22,23] In the case of strong coupling, the interaction of associated electrons can also be adjusted, which greatly increases the freedom of device adjustment. At low temperatures, measurements with extremely high energy resolution have observed very fine gate-dependent physical effects, such as the Coulomb blockade, Kondo effect and electron–phonon coupling.[24–26] It can provide rich information on the molecule, including electronic transitions between energy levels, molecular vibrations and changes in spin states. Furthermore, some molecular-scale physical effects can be controlled by specially constructing single-molecule FETs, including quantum interference, spin, thermoelectric effects, superconductivity, and so on.[8,27–30] Therefore, specific applications can be achieved using single-molecule devices.[8,9,11]

In this review, we present the research progress in single-molecule FETs with solid or liquid gates. The first part is about the design and construction of single-molecule FETs; the second part is about the basic mechanisms of single-molecule FETs; the third part is about the applications of single-molecule FETs; at the end, the current opportunities and challenges in the field of single-molecule FETs are proposed, aiming to promote the future development of single-molecule electronics.

2. Design and construction of single-molecule FETs

The construction of single-molecule electronic devices is a promising approach to overcome Moore's law and improve the integrated circuit technology.[31–35] In comparison with two-terminal molecular devices, single-molecule FETs, in which a single molecule acts as the tunable charge transport part in three-terminal device configurations, are the key components for further integration of molecular-level electronic circuits. According to the types of gates, such as solid and liquid gates, and generalized gates with external stimuli, we divide single-molecule FETs into three categories in this review. Single-molecule FETs with solid gates have potential applications in integrated circuits. Liquid gating with large gate adjustment capabilities is an alternative method to understand the charge transport characteristics of single molecules. While based on the two-terminal device, the introduction of external stimuli as a generalized gate provides a new concept for the design of novel single-molecule FETs.

2.1 Single-molecule FETs with a solid gate

The fabrication of nanogap electrodes is the basis for constructing single-molecule FETs.[36] Specifically, the effective distance of the nanogap between the source and drain electrodes is expected to match the length of the molecule to form a single-molecule junction. How to construct a solid gate electrode to effectively apply a gate electric field to a single molecule in the nanogap is another key to construct single-molecule FETs. The gate coupling parameter β is used to estimate the shift degree of the orbital levels of the molecule with the gate potential. Since the shielding of the gate potential by the source/drain electrodes will reduce the parameter β, the geometry of the nanogap electrodes needs to be considered. Therefore, considering the above key points, applicable approaches for fabricating nanogap electrodes with solid gates should be developed, so that the construction of single-molecule FETs involves fewer processes or minor modifications.

Chuancheng Jia

Prof. Chuancheng Jia received his PhD degree in 2014 from the College of Chemistry and Molecular Engineering, Peking University, under the guidance of Prof. Xuefeng Guo. From 2014 to 2020, he was a postdoc at the Institute of Chemistry, Chinese Academy of Sciences and University of California, Los Angeles. He joined the faculty as a professor at Nankai University in 2020. His research is focused on single-molecule electronics and dynamics.

Xuefeng Guo

Prof. Xuefeng Guo received his BS degree in 1998 from Beijing Normal University and his PhD degree in 2004 from the Institute of Chemistry, Chinese Academy of Sciences, Beijing. From 2004 to 2007, he was a postdoc at the Columbia University Nanocenter. He joined the faculty as a professor under the "Peking 100-Talent" Program at Peking University in 2008. His current research is focused on functional nanometer/molecular devices.

2.1.1 Electromigration junction-based single-molecule FETs. The most common strategy for fabricating single-molecule FETs based on single-molecule break junctions is to form nanogap electrodes by electromigration breaking.[37] When a high-density current is applied to an unbroken thin and narrow metal wire, the metal atoms undergo electromigration in the conductor, which eventually causes the metal wire to break. The size of the electromigration nanogap can be as small as the molecular level to trap a single molecule, so that a single molecule can be bridged stochastically with a high probability. In addition, it is feasible to integrate electromigration nanogap electrodes on a Si wafer, so the gate coupling can be enhanced by placing single-molecule junctions directly on gate dielectrics.

The first single-molecule FET was fabricated in 2000, which introduced a single C_{60} molecule to bridge nanogap Au electrodes fabricated by the electromigration break junction technique.[1] When a voltage is applied to the SiO_2 insulating layer through the gate electrode, the current of single C_{60} molecule junctions can be regulated. To further improve the gate control ability, electron beam lithography is used to fabricate nanogap Au source/drain electrodes on the aluminum gate electrode pad, which is covered with a $\sim$3 nm oxide layer as a dielectric layer. Then, a single divanadium (V_2) molecule is connected into nanogap Au electrodes to fabricate a single-molecule FET (Fig. 1a).[38] The Kondo resonance of the single-molecule FET can be observed, which can be modulated reversibly through the gate voltage to change the charge and spin states of the divanadium molecule. In addition, magnetic metals can also be used as nanogap electrodes to construct single-molecule FETs instead of gold electrodes, which provides a potential platform to study the spin-dependent transport characteristics. Single C_{60} molecule FETs with 15 nm thick ferromagnetic Ni leads have been constructed (Fig. 1b),[39] which were fabricated on a 100 nm thick oxide layer grown on heavily p-type doped Si substrates by using electron-beam lithography and electron-beam evaporation. When Ni nanogap electrodes are designed to have an asymmetrical shape, the single-molecule device may undergo magnetic reversal under different magnetic fields due to shape anisotropy. When source/drain electrodes are replaced with superconducting materials, superconducting research of single-molecule FETs can also be investigated. For instance, a superconducting single C_{60} molecule FET is fabricated by the electromigration technique,[40] in which the superconducting contact with the C_{60} molecule is made of aluminum or gold, and the superconductivity is induced by the close vicinity of the aluminum capping layer. At the dilution refrigeration temperature, the electrical characteristics of superconducting single-molecule FETs can be accurately measured. In single-molecule FETs with solid gates fabricated using the electromigration technique, various new properties of single molecules, such as the Coulomb blockade, Kondo effect, superconductivity, resonant coherence and incoherent tunnelling, can be explored.

2.1.2 Mechanically controllable break junctions-based single-molecule FETs. Another method to create nanogap electrodes is the mechanically controllable break junction (MCBJ) technique,[41] which shows the precisely controllable gap size through the bending of the substrate. Specifically, the bending of the substrate can be achieved *via* a three-point bending configuration, which will eventually lead to stretching and breaking of the electrode wire (Fig. 1c).[65] The formed nanoscale gaps can be used for the electrical contact of single molecules, such as assembly from solution.[12]

Single-molecule FETs can be realized through the MCBJ technique in combination with electrostatic gating and mechanical regulation.[12] A degenerately doped silicon substrate is used as a bottom gate electrode, which makes it possible to produce molecule-gate spacing as small as 40 nm through electron beam lithography. However, the brittleness of the Si substrate during mechanically controllable break limits the movement range of the electrode. A sandwich-type gated MCBJ is further constructed on a phosphor bronze substrate, and the Au electrode is directly deposited on the plasma alumina gate, which avoids an unnecessary gate field electromechanical effect in the suspending source–drain electrode device.[42] This three-terminal MCBJ not only accurately controls the distance between two electrodes, but also ensures a high coupling between the molecule and the gate. With a high k dielectric layer, gate coupling can be further improved. For the overlap of the gate electrode and nanogap electrode, high-precision alignment is required to achieve as small as 1 μm^2, thereby significantly reducing the leakage current path through the oxide. Three different gate dielectrics, plasma-enhanced AlO_X (4 nm), SiO_2 (10 nm) and Ta_2O_5 (10 nm), are tested, respectively. The Ta_2O_5 dielectric layer shows superiority with a dielectric constant of about 24–28, a low leakage current of below $\pm$1 pA and a high gate voltage of up to $\pm$5 V at room temperature.[43] The electromigration assists the mechanical break process to prevent the dielectric layer from splitting, and good electrostatic regulation can be achieved. In addition, Xiang *et al.* introduced a non-contact side gate into the MCBJ

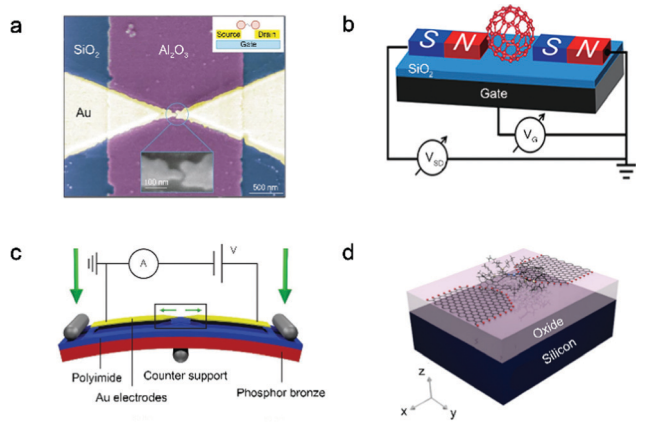

Fig. 1 (a) Single-molecule FET incorporating single divanadium molecule.[38] Copyright: 2002, Nature Publishing Group. (b) Single C_{60} molecule FET with ferromagnetic Ni electrodes.[39] Copyright: 2013, American Chemical Society. (c) Layout of the MCBJ set-up.[65] Copyright: 2013, Macmillan Publishers Limited. (d) Schematic diagram of a single-molecule transistor with a back gate and graphene nanoelectrode.[49] Copyright: 2015, The Royal Society of Chemistry.

(Fig. 1c) to form a stable three-terminal single-molecule FET.[14] The perpendicular distance between the gate and single-molecular junctions is reduced to about 5 nm, which can simultaneously shift the molecular energy levels and modulate the molecular charge transport.

2.1.3 Carbon electrode-based single-molecule FETs. For single-molecule devices with metal electrodes, the high mobility of gold atoms leads to relatively unstable single-molecule junctions at room temperature. Carbon-based electrodes,[44,45] especially graphene electrodes, with stable characteristics are supposed to be an alternative choice, and they also match well with organic molecules. It is feasible to create nanoscale gaps and covalently or non-covalently connect single molecules to graphene electrodes with more defined binding geometries. In this review, we focus on graphene electrodes, considering the sensitivity of carbon nanotube electrodes to gate voltages, which might hamper us to understand the intrinsic properties of single molecules in FETs.[2,7]

Some theoretical studies have been reported to predict the construction of single-molecule FETs using the nanogapped graphene electrodes.[46] Different from the principle of traditional single-molecule FETs, the field effect of the graphene-based single-molecule FETs can be achieved by regulating both graphene electrodes and molecules through the gate. Furthermore, in comparison with bulk metal electrodes, thin graphene-based electrodes can reduce the shielding effect on the gate electric field and enhance the gate coupling. The use of graphene-based electrodes can also solve the problem of size mismatch between single molecules and electrodes. In addition, in comparison with metal electrodes, single molecules can be connected to graphene electrodes in a variety of ways, not only through π–π stacking,[47] but also through covalent bonds.[48]

Nanogapped few-layer graphene electrodes have been fabricated by using feed-back controlling electroburning.[47] The few-layer graphene is chosen because its conductance is not adjusted by the gate, thereby avoiding the characteristics of the connected single molecules from being affected by the response of the electrode to the gate. In addition, with chemical vapor deposition (CVD) grown single-layer graphene, nanogapped electrodes prepared by an electroburning method and π–π stacking molecule-electrode connections are used to construct single-molecule FETs (Fig. 1d).[49] Such single-molecule junctions are insensitive to the atomic configuration of the electrodes and show good reproducibility. However, the gate response characteristics of the CVD grown single-layer graphene electrodes have not been verified, and the influence of the electrodes on the single molecular characteristics during the test cannot be ruled out. The local buried bottom gate can directly electrostatically modulate the molecular orbitals in the single-molecule FETs, and achieve a relatively high modulation efficiency. However, in previous studies, the effect of gating the state density of the graphene electrode is usually ignored. Sun *et al.* realized the regulation of the Dirac-cone of graphene electrodes in the single-molecule junction by a local gate.[50] Specifically, a local aluminum pad with a naturally oxidized alumina layer is used as the gate. A 10 nm thick HfO_2 dielectric layer is grown by atomic layer deposition, which can avoid destroying the traditional Al_2O_3 dielectric layer during the introduction of wet graphene. In comparison with the non-local SiO_2/Si bottom gate, the local HfO_2/Al_2O_3/Al bottom gate has a higher gate efficiency.

2.2 Single-molecule FETs with a liquid gate

Although single-molecule FETs have been studied for many years, there are still many challenges in preparing devices, especially with solid gates. Several things are needed to be considered for an ideal single-molecule FET: (1) the distance between the gate electrode and the molecule should be as small as possible in order to generate a large enough electric field, which is difficult to achieve in the solid state; (2) the shielding effect of the source–drain electrodes to the gate electric field should be minimized. The shielding effect will be enhanced as the distance of source–drain electrodes is smaller than that between the gate electrode and the molecule, while the distance between the source and drain electrodes is dependent on the length of molecule. These requirements are difficult to be met for single-molecule FETs controlled by solid-state electrostatic gate. However, single-molecule FETs with liquid ion gates can make up for the shortcomings of solid-state FETs, can operate in a liquid ion environment and achieve high gate efficiency.[5,51,52] Single-molecule FETs with liquid gates can modulate molecular conductance through direct orbital gating or electrochemical electron transfer driven by the ionic double-layer potential.

For instance, Xu *et al.* have used a scanning tunnelling microscopy (STM) technique and perylene tetracarboxylic diimide (PTCDI) as redox functional molecules to construct single-molecule junctions.[53] Due to the molecular-level thickness of the ion double layer at the electrode–electrolyte interface, a large gate electric field can be applied to single-molecule junctions by using an electrochemical gate in the electrolyte. Single-molecule electrochemical transistors based on 4,4′-bipyridine with Ni and Au contacts have also been established (Fig. 2a),[54] in which electrochemical control is utilized to prevent oxidation of Ni contacts and to provide non-redox electrochemical gating of the devices. The results reveal that, in comparison with Au electrodes, Ni electrodes in single-molecule devices display significant advantages, especially due to the influence of Ni d-electrons, which leads to larger conductance and more stable chemical binding.

Aqueous solutions are usually used as electrolytes, but they will condense during low temperature measurements, which limits their further applications. The ionic liquid is considered to be an ideal candidate for gating because it has higher electrochemical stability and a larger potential window, and can achieve gating modulation under low-temperature vacuum conditions. For instance, based on an STM technique, the electrical properties of a single redox active pyrrolo-tetrathiafulvalene (pTTF) molecule have been studied in a single-molecule device with ionic liquid electrochemical gating at room temperature (Fig. 2b).[13] When the electrochemical potential is scanned from positive to negative potentials through redox transitions, an ''off–on–off–on–off'' conductance switch behaviour is realized. This is due to a sequential

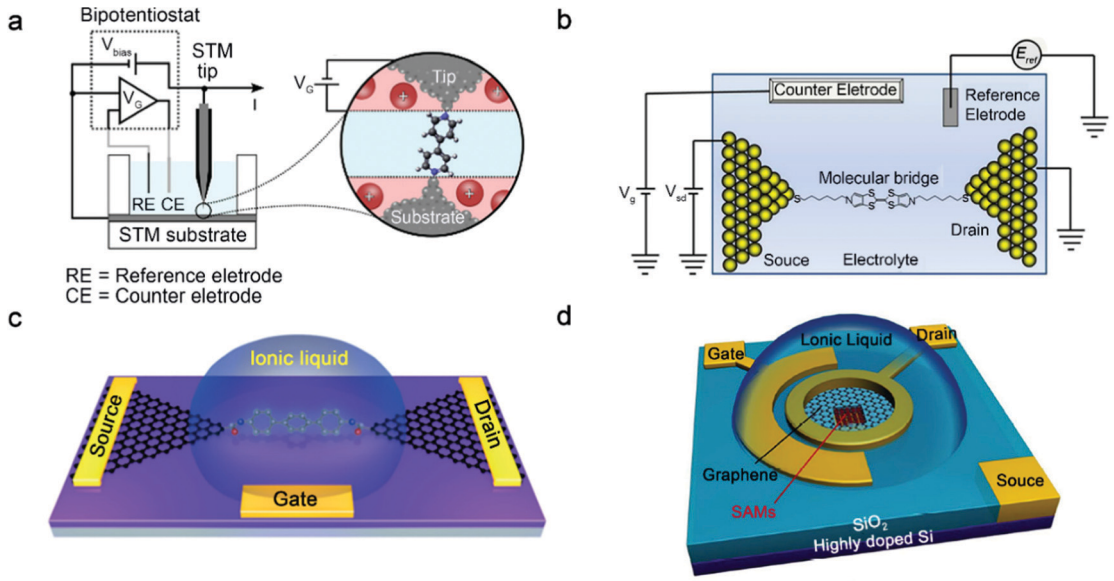

Fig. 2 (a) Schematic diagram of the four-electrode cell for electrochemical single-molecule junctions and the electrochemical double layer over the junction which the gate voltage (V_G) is applied.[54] Copyright: 2014, American Chemical Society. (b) Schematic diagram of an electrochemical single-molecule junction with electrolyte gating.[13] Copyright: 2012, American Chemical Society. (c) Schematic illustration for the setup of single-molecule FETs with graphene nanogap electrodes and ionic liquid gate.[55] Copyright: 2018, Wiley-VCH Verlag GmbH & Co. KGaA, Weinheim. (d) Schematic diagram of the vertical molecular tunneling transistor with an ionic liquid gate.[58] Copyright: 2018, American Association for the Advancement of Science.

two-step charge transfer process with full or partial vibration relaxation. In addition to single-molecule junctions with metal electrodes, a series of single-molecule FETs (Fig. 2c) based on graphene–molecule–graphene single-molecule junctions with an ionic-liquid gate have also been constructed.[55] Experimental and theoretical results reveal that ionic liquid gating can modulate the energy level alignment between molecular frontier orbitals and the Fermi energy level of graphene electrodes.

Cross-plane graphene/self-assembled monolayer (SAM)/gold molecular tunnelling junctions with ionic liquid gating (Fig. 2d) have also been constructed and operated at room temperature.[56–58] A strong gating electric field could be generated from the electrical double layer of ionic liquid after applying the gate voltage. Due to the partial electrostatic transparency of graphene, the electric field can penetrate through the graphene layer and tune the energy levels of single molecules in SAM, which would achieve an effective current modulation of molecular FETs. Further results demonstrate that the transistor exhibits a high on–off ratio due to the destructive quantum interference (QI) characteristics of the molecule. The destructive QI effects discovered in single molecules might provide an opportunity to design new devices with high performance. Molecular transistors operate in the quantum tunnelling regime, providing potential electronic building blocks for future integrated circuits.

2.3 Generalized single-molecule FETs with other gates

In general, a typical single-molecule FET is an electronic component, which has at least three terminals including a gate electrode, and is used as an amplifier or an electrical switch according to its characteristics. The charge transport of single-molecule junctions can be modulated not only by gates, but also by other strategies, such as light, magnetic field or functional group modification. This can be regarded as generalized gate modulation relative to typical gates. In addition, the comprehensive multiple effects of generalized gates will enhance the understanding of basic physical mechanisms at the single-molecule level and help to develop multifunctional devices.

The switching behaviour is commonly pursued in a single-molecule device due to its potential application in logical devices and memories. For instance, Yu *et al.* have used chemical modification to achieve a switching effect in the single-molecule junction, which contains an edge-on pyridino-paracyclophane moiety triggered by the protonation of the pyridine ring.[59] Protonation converts single-molecule charge transport from p-type to n-type. The switch mechanism is attributed to the change of the charge tunnelling channel from the highest occupied molecular orbital (HOMO) in a neutral molecule to the lowest unoccupied molecular orbital (LUMO) in a protonated molecule, thus forming a binary system. A further work based on pyridinoparacyclophane acting as diodes was developed, which demonstrates that the rectification ratio can be enhanced by a through-space gating effect as the increasing electron-rich gating group (Fig. 3a).[60] This phenomenon might result from a shift in the HOMO level both spatially and energetically. Photoisomerization of photochromic molecules can form two different conformational and electronic states, which provides a broad prospect for building logic and memory devices at the single-molecule level. For instance, single diarylethene molecules are covalently connected to nano-gapped carbon electrodes to form single-molecule junctions.[61,62] For the single diarylethene molecule junctions based on carbon nanotube electrodes,[63] since energy is transferred from the photoexcited

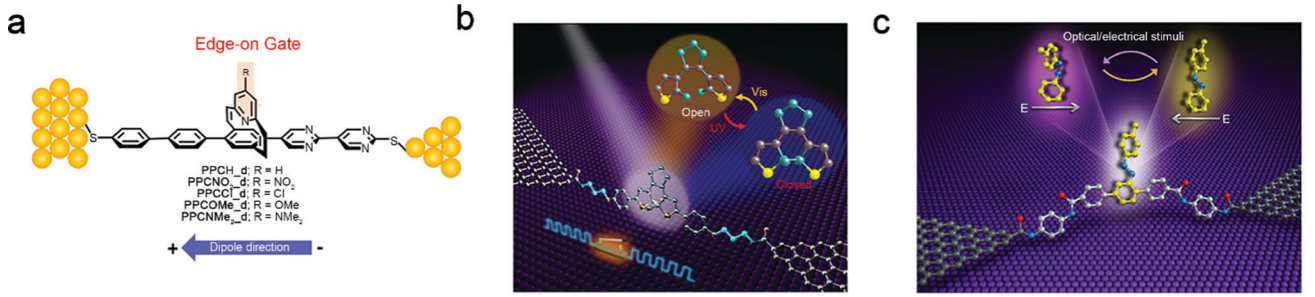

Fig. 3 (a) Assembly of pyridinoparacyclophane based diodes with edge-on gates on the Au surface.[60] Copyright: 2016, American Chemical Society. (b) Schematic of a graphene–diarylethene–graphene junction.[61] Copyright: 2016 by the American Association for the Advancement of Science; (c) schematic representation of the single-molecule junction with an azobenzene side group as a chemical gate.[64] Copyright: 2019, Springer Nature Limited.

diarylethene molecule to the extended π-electron system of the carbon electrodes, an irreversible "off–on" switch can be observed, which indicates that it cannot be isomerized from the closed form back to the open form under visible irradiation. In order to achieve the reversible switching effect in the graphene-based single-molecule junctions, various molecular designs are considered to adjust the energy level alignment and electronic coupling at the molecule–electrode interface. When three CH_2 units are introduced to each side of the molecular backbone to optimize the molecule–electrode coupling, the reversible light-controlled conductance switch is realized in the single-molecule devices (Fig. 3b).[61] In addition, a reversible azobenzene-based single-molecule photoswitch device was also designed by making use of light- and electric field-driven *cis–trans* isomerization of the azobenzene molecular functional center.[48] Specifically, an azobenzene molecular bridge is covalently incorporated between the nano-gapped graphene electrodes through the amide covalent linkage (Fig. 3c).[64] To avoid the quenching of the excited state of the molecule, the azobenzene moiety is introduced as the side chain of the molecular bridge, and the molecular backbone with benzene rings is used for charge transport. Both experimental and theoretical investigations demonstrate that the switching behaviour can be easily detected under different source–drain bias voltages or at low bias voltages under UV/Vis light irradiation. This concept of *in situ* chemical gating provides a new perspective for the practical creation of multifunctional single-molecule optoelectronic devices. Therefore, multifunctional single-molecule transistors can be constructed not only by the gate electric field modulation, but also by external stimuli based on molecular structural changes.

3. Mechanisms of single-molecule FETs

In order to better design and construct single-molecule FETs, it is necessary to deeply understand the mechanism. The essential mechanism of single-molecule FETs is to control the relative position of the molecular orbitals with the Fermi level of the electrodes through the gate electric field. The molecule–electrode interface coupling determines the mode of charge transport through single molecules. Therefore, the interface coupling mechanism of the single-molecule FETs is first introduced below. To better understand the charge transport behaviour of single-molecule FETs, the Coulomb blockade effect, Kondo effect and electron–phonon coupling effect are discussed in detail.

3.1 Molecule–electrode interface coupling

Electrons inject molecules from one electrode through the interface, and then across to the other electrode from the interface. Therefore, the interface between the molecule and the electrode plays an important role in the transport characteristics of the molecular device.[65] Through the experiments of single-molecule FETs to explore the properties of the interface between molecules and electrodes, it is found that the influence of the interface between molecules and electrodes on device characteristics even exceeds that of molecules.[21]

The interfacial coupling strength is an important parameter that determines the transport mechanism of single-molecule devices. In order to better define the coupling strength, it is necessary to introduce two energy concepts: one is the energy required for the additional energy (U_{add}) molecule to increase or decrease an electron, and the other is the coupling energy. When molecules are connected to electrodes, the energy levels of discrete molecules that are originally under weak coupling or isolation will broaden, and this broadening is represented by coupling energy (Γ). When $\Gamma \ll U_{add}$, it is weak coupling; when $\Gamma \gg U_{add}$, it is strong coupling; between the two is called intermediate coupling (Fig. 4a and b).[20] Using the gate to control the electron transport through single-molecule devices, the energy levels of the molecules can be adjusted to resonate with the Fermi level of source and drain electrodes. In a three-terminal device with strong coupling, it is predicted to be a one-step coherent electron transfer. However, weak coupling promotes a two-step process, such as Coulomb blockade. Many electron–electron correlation effects can be observed under the transition coupling mechanism, such as the Kondo effect and incoherent tunnelling.

There are two main types of contact between molecules and electrodes. One is chemical adsorption with covalent bonds, and the other is physical adsorption. In comparison with physical adsorption, chemical adsorption can lead to stronger coupling strength. This is mainly determined by the electrode type and the anchor group at the end of the molecule. Whether

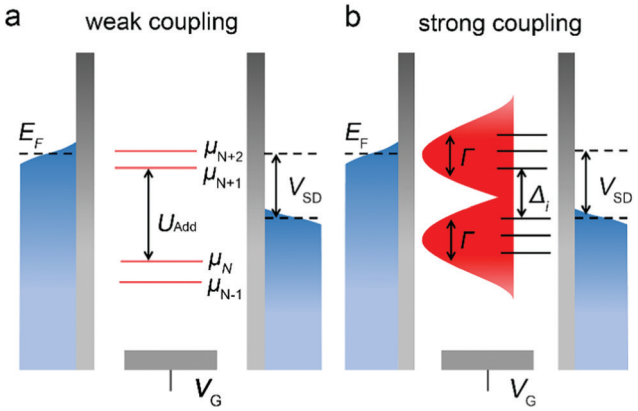

Fig. 4 (a) Schematic diagram of energy levels in a single-molecule junction under weak coupling and (b) strong coupling.[20] Copyright: 2009, Macmillan Publishers Limited.

it is chemical connection or physical connection, changing the anchor group will affect the charge transfer. In other words, the anchor group affects the charge transfer through some internal factors, that is, the coupling strength. Even if the adsorption type is the same, if the coupling strength is different, the transport characteristics of single-molecule FETs will be different. For example, using MCBJ and STM-BJ to electrochemically gate single benzodifuran (BDF) molecules with redox activity through the chemical connection to the electrodes, it is found that the sulfur-terminal BDF molecules exhibit single-molecule redox switching characteristics by adjusting the potential. If the sulfur end group is changed to carbodithioate (CS_2^-), as shown in Fig. 5a, the molecular conductance increases. During the gating process, the on–off ratio is also significantly increased, as shown in Fig. 5b, indicating that the gate effect can be improved by reducing the resistance between the molecule and electrodes.[66] This proves that the gate regulation will be affected by the coupling strength in the case of a chemical connection. For the case of physical connection, Limburg *et al.* have used porphyrin molecules with five different types of anchoring groups, as shown in Fig. 5c, which can be connected to graphene electrodes by physical adsorption (Fig. 5d). Because of the weak coupling, all devices exhibit the behaviour of single electron FETs. The differences in electron transport characteristics for the devices with these five anchor groups can be compared by the difference of Coulomb peaks. However, since the complex of each molecule and the anchor group leads to a large range of changes in the coupling strength, as shown in Fig. 5e, the position of the Coulomb peak is also different in different devices. Although it is difficult to distinguish the effects of these types of anchor groups on the charge transport through different devices, the number of Coulomb peaks can also be used to distinguish the anchor groups with large differences.[67]

3.2 Energy level shifting

Single-molecule FETs rely on gated electrostatic modulation of the relative position of the molecular orbitals with respect to the Fermi level of the electrode. Creating a true three-terminal single-molecule device that operates in this way is a long-standing challenge. Different from the two-terminal device, in addition to fixing the molecules on the source and drain electrodes, the molecules must be close enough to the gate to ensure that the gate electric field can act on the molecules.

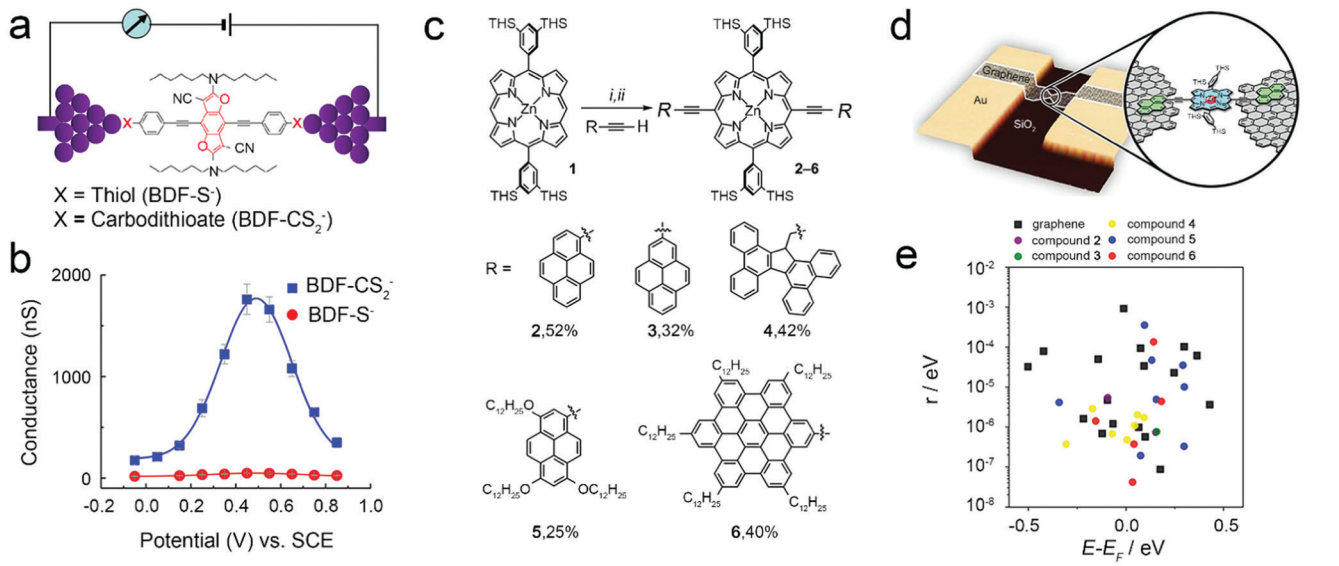

Fig. 5 (a) Schematic of a single-molecule junction of a BDF molecule with thiol ($-S^-$) or carbodithioate ($-CS_2^-$) anchoring groups. (b) Single molecule conductance of BDF-S^- (red circles) and BDF-CS_2^- (blue squares) as a function of gating.[66] Copyright: 2014, American Chemical Society. (c) Synthesis of zinc porphyrins 2–6 from molecule 1 with different terminal groups. THS = trihexylsilyl. i. *N*-Bromosuccinimide, $CHCl_3$, pyridine, 20 °C, 98%. ii. Sonogashira coupling conditions with RC≡CH, 25–52%. (d) Schematic of the single-molecule device with nanogap graphene electrodes and assembled single molecule. (e) Scatter plot of the coupling to the leads *versus* the energy of the resonant level relative to the Fermi level ($E - E_F$).[67] Copyright: 2018, WILEY-VCH Verlag GmbH & Co. KGaA, Weinheim.

For instance, Xu *et al.* achieved an experimental breakthrough for the first time, using the perylene tetracarboxylic diimide (PTCDI) molecule to construct a single-molecule FET with a liquid gate. A single-molecule n-type transistor is realized, in which at room temperature the current through the molecule can be reversibly switched over nearly 3 orders of magnitude through electrochemical gating. One mechanism is resonant tunnelling, which predicts that the current reaches a peak when the empty molecular orbital is shifted by the gate to the Fermi level of the electrodes.[53] It is also proved that the electrochemical gate modulates the relative position of the molecular orbital relative to the Fermi level in the non-electrochemically active potential range.[68] Due to the high efficiency of the electrochemical gating, in the process of adjusting the relative position of the molecular orbital respect to the Fermi level, both the HOMO and LUMO dominated electron and hole transport can be achieved, respectively (Fig. 6a). When the energy gap between the HOMO and LUMO is small, the single-molecule FETs can achieve bipolar transport (Fig. 6b and c).[19,55,69]

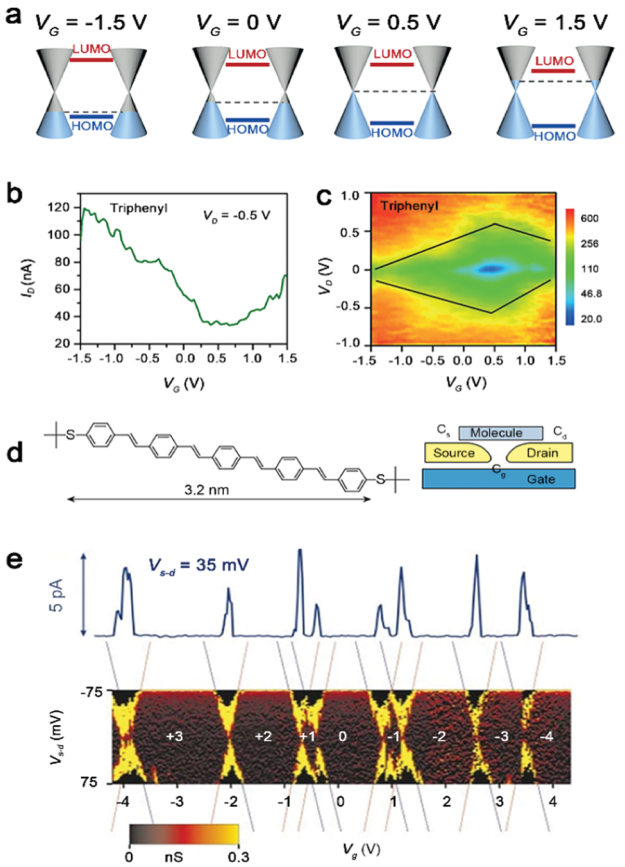

Fig. 6 (a) Energetic diagram of the alignment of molecular orbitals relative to the graphene Fermi level in a triphenyl single-molecule FET under different gate voltages. (b) Transfer characteristics for the triphenyl device at V_D = 0.5 V. (c) Two-dimensional visualization of d*I*/d*V* *versus* V_G and V_D for the triphenyl device.[55] Copyright: 2018, Wiley-VCH Verlag GmbH & Co. KGaA, Weinheim. (d) Molecular structure of OPV5 and schematic experimental set-up. (e) Measurements of the differential conductance (dI_{s-d}/dV_{s-d}) as a function of V_{s-d} and V_g. The full solid line at the top of the figure shows a representative I_{s-d}–V_g trace.[71] Copyright: 2003, Nature Publishing Group.

Furthermore, single-molecule FETs are also realized through the direct electrostatic shift of energy levels of the molecular orbitals in a solid-state device with a back gate electrode.[22] However, Xiang *et al.* also found that in single-molecule FETs composed of BDF molecules, the charge transfer under low bias voltages is mainly affected by the coupling strength between molecules and electrodes, while the influence of the gate voltage is very weak.[70]

3.3 Coulomb blockade effect

In the case of weak coupling, the obvious Coulomb blockade can be realized in single-molecule FETs. The electrons pass through the molecule one by one, which is a typical quantum phenomenon. Specifically, when the device size is reduced to the molecular scale, the Coulomb interaction between the electrons is enhanced, so that when an electron enters the molecule, the next electron will not be able to enter the molecule due to insufficient energy. By increasing the source–drain voltage or adjusting the gate voltage, electrons can break through the Coulomb blockade and enter the molecule. Adjusting the gate voltage can change the energy level position of the molecular orbital, thereby reducing the energy difference between the molecular orbital and the Fermi level. After the molecular orbital enters the bias window, electrons can undergo resonant tunnelling. This process is performed in a manner of continuous tunnelling of a single electron. Therefore, such single-molecule FETs are also called single-electron FETs. For instance, a single-molecule FET is constructed by using a single *p*-phenylenevinylene oligomer to protect the terminal sulfur through a *tert*-butyl group to prevent the chemical adsorption of sulfur with the gold electrode, as shown in Fig. 6d, thus the physical adsorption between the molecule and the electrode is realized for weak coupling. The single electron tunnelling process can be observed in this single-molecule FET with weak interfacial coupling. Specifically, through the electrical test with the gate voltage in the range of −4.3 to 4.3 V, eight different charge transport states as shown in Fig. 6e can be observed.[71] When a Coulomb blockade occurs, a Coulomb diamond shape will appear on the electrical spectrum. Therefore, each Coulomb diamond shape corresponds to a charge state. The intersection of the two diamond shapes is the degeneracy point of the charge, and redox occurs at this position.

3.4 Kondo effect

When the coupling strength between the molecule and the electrode is weak, electrons can only tunnel through one barrier at a time, and the current is formed by the continuous tunnelling of a single electron. However, when the coupling strength between the molecule and the electrode increases, the high order tunnelling process of electrons begins to appear, which is related to the electron spin called the Kondo effect.[72–75] The most widely studied Kondo process for single-molecule FETs is the single-channel Kondo effect with spin 1/2 (Fig. 7a), that is, the system containing a single magnetic center. Due to the Kondo effect, the density of states of the electrons near the Fermi surface is significantly enhanced, which appears as a clear resonance conductance peak at zero bias.

The Kondo effect only occurs when the coupling strength between the molecule and the electrode is strong enough. For instance, cobalt complex molecules are connected to metal electrodes through insulating tethers with different lengths to construct single-molecule FETs. By changing the length of the insulating tethers, the coupling strength between the molecules and the electrodes can be changed. When the insulating tether is long, it behaves as a single electron FET (Fig. 7b); when the insulating tether is short, the Kondo effect appears. The single-molecule junctions composed of cobalt complexes can exhibit both the Kondo effect and the Coulomb blockade effect at the same time when the interfacial coupling is intermediate, and the charge state can be adjusted by the gate voltage. When in the Co^{2+} state, the total spin quantum number S = 1/2, and the Kondo effect will appear in this case (Fig. 7c). Such a Kondo effect is usually expressed by the Kondo temperature T_k. In the cobalt complex system, the Kondo temperature can reach up to 25 K.[38] While for the single-molecule FET with a divanadium molecule, the Kondo temperature can reach up to 30 K.[24] When the temperature is lower than T_k, the Kondo effect occurs, the conduction electrons are scattered, and the local spins are constantly flipped, showing that the conduction electrons shield the local spins. When the temperature is lower, the shielding effect is stronger. At absolute zero, the local spin is completely shielded.

3.5 Electron–phonon coupling effect

Electron–phonon coupling indicates that when electrons pass through molecules, they absorb or release a quantum of energy, usually called phonon. The charge transport channel length of single-molecule FETs is usually on the order of sub-nanometers, which is smaller than the inelastic mean free path of electrons. It is believed that most electrons pass through the single-molecule device by elastic scattering, and little inelastic scattering occurs. Therefore, electron–phonon coupling is usually ignored in the early research of single-molecule FETs. With the deepening of research, the influence of electron–phonon interactions on the electron transport of single-molecule FETs has gradually attracted attention.[25,27,76,77]

In the case of weak coupling, molecules can change the ground state by gaining and losing electrons. This process involves the Franck–Condon mechanism. When the charge and vibration are strongly coupled, the Franck–Condon blocking effect will appear. For instance, Burzurí *et al.* show the experimental evidence of the FC blockade effect in electron transport *via* an individual magnetic molecule ($[Fe_4(L)_2(dpm)_6]$). It suppresses the single electron tunnelling process under a low bias voltage and is not controlled by the gate voltage. As shown in Fig. 7d, under the bias below the threshold V_{th} = ±7.4 meV, sequential electron tunnelling is highly suppressed. When the electron–vibron coupling λ is strong, the zero-bias conductance suppression may originate from the FC blockade effect (Fig. 7e).[28,78] In the case of intermediate coupling, the tunnelling process is accompanied by vibration excitation or de-excitation through the virtual state of the molecule. When the bias voltage increases and the energy of the electron exceeds the energy difference between the two vibration modes, a new transport channel will be opened to increase the charge transport (Fig. 7f).

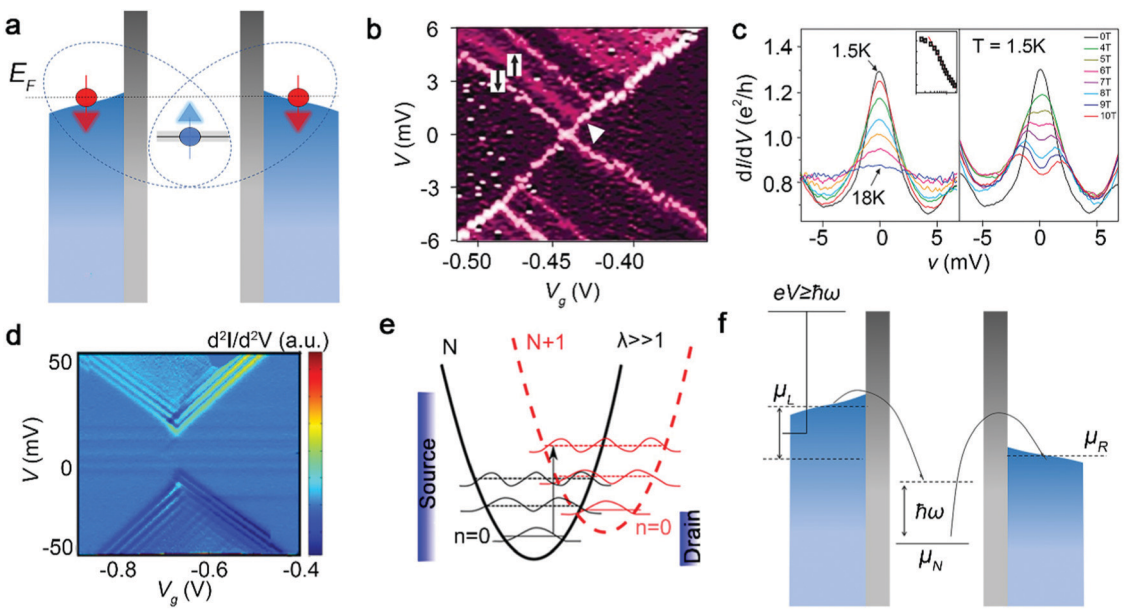

Fig. 7 (a) Schematic of the mechanism of the spin 1/2 Kondo effect. (b) Differential conductance diagram of the spin signal is superimposed on the Coulomb blocking signal. (c) Typical temperature dependence of the Kondo peak (left) and magnetic-field dependence of the Kondo peak (right) for the single-molecule device with spin electron.[38] Copyright: 2002, Nature Publishing Group. (d) Numerical derivative of differential conductance (d^2I/d^2V) color map as a function of bias V and gate voltage V_g for the single-molecule junction with periodic excitations. (e) Schematic representation of the Franck–Condon model for strong electron–phonon coupling.[78] Copyright: 2014, American Chemical Society. (f) Schematic of the electron–phonon coupling effect in the case of intermediate coupling.[79] Copyright: 2019, Springer Nature Limited.

In the case of strong coupling, the emission of the vibration mode will increase the backscatter and suppress the increase in current.[79]

4. Applications of single-molecule FETs

By constructing and designing different types of single-molecule FETs, the regulation of quantum interference, spin, thermoelectricity and superconductivity can be achieved at the single-molecule level.[9,29,77,80–82] This will help to understand the essential physical mechanism of these physical properties and realize the construction of high-performance functional devices. Single-molecule FETs also have many applications in bioelectronics, which can be obtained from recently published review papers.[83,84] The following section will focus on the applications related to physical mechanisms. The following will introduce the regulation of these effects in single-molecule FETs.

4.1 Regulation of the quantum interference effect

The quantum interference of single-molecule devices describes the interference effects of tunnelling electrons through a single molecule. Due to the uniqueness of sub-nanoscale single-molecule devices, electrons can maintain quantum coherence when they transport through single molecules, making it possible to study quantum interference in the process of electron transport.[85,86] The quantum interference in the single-molecule FETs can control the transmission coefficient, which is one of the effective means to achieve high-efficiency control. Therefore, controlling the quantum interference effect is an important means to realize the function of the single-molecule FETs with the quantum interference effect.

Single-molecule FETs can control the quantum interference effect either through redox or through adjusting the relative position of the molecular orbital with the Fermi level. For instance, Koole *et al.* realized the regulation of quantum interference by using single-molecule FETs to control the redox states of the molecule. Specifically, anthraquinone (AQ) molecules with the quantum interference effect are used to construct single-molecule FETs. By controlling the gain and loss of electrons of the AQ molecule, an order of magnitude of conductance switching effect can be achieved in a single-molecule FET. This is due to the changes in the conjugation of the AQ molecule during the redox process, which changes the quantum interference path, resulting in a high switching ratio.[87] In 2018, Huang *et al.* used the single-molecule field effect mechanism to realize the regulation of quantum interference. For the single-molecule junctions with *meta*-benzene (*meta*-BT) (Fig. 8c) based molecules and dihydrobenzo[*b*]thiophene as the anchoring group, more than two orders of magnitude changes in conductivity can be observed during the electrochemical gating process. The electric potential modulates the quantum interference of the *meta*-BT molecule to make it enter anti-resonance, so that the sharp-valleyed quantum interference effect can be directly observed.[88] Subsequently, Duan, Tao and Hong's research groups also used an electrochemical gate to directly observe the distinctive features of destructive quantum coherence in molecules with quantum interference properties (Fig. 8a).[56,58,89,90] When adjusting the electrochemical gate in the Faraday zone, the relative position of the molecular orbital with the Fermi energy level can be adjusted to modulate the quantum interference between the HOMO and LUMO (Fig. 8b). Since the molecules can enter and exit anti-resonance, they can achieve continuous control of conductance. Therefore, the quantum interference effect can be regulated by the gate control of the molecular charge states or the molecular energy level position, thereby improving the switching performance of the single-molecule FETs.

4.2 Regulation of the spin effect

The regulation of the spin state in magnetic molecules is the focus of spintronics research, especially the regulation of the spin through the electric field.[91,92] Unlike the magnetic field, the electric field can achieve faster regulation in a more local space. The single-molecule FET provides an ideal means to adjust the spin state of a single magnetic molecule through an electric field. For instance, the transition from high spin ($S = 5/2$) to low spin ($S = 1/2$) is realized in a single-molecule FET constructed by a single Mn^{2+} ion coordinated by two terpyridine ligands through electric field control, as shown in Fig. 8d. This transition is realized by the modulation of the terpyridine ligand by the gate electric field. By increasing the gate voltage, a spin 1/2 electron can be added to the terpyridine ligand, thereby enhancing the intensity of the ligand field and realizing the transition of Mn center from high spin to low spin.[23] The modulation of the spin state by the electric field can be achieved not only in transition metal complexes, but also in free radical molecules. For instance, the regulation of the spin state by the electric field is realized in single-molecule FETs with the all-organic free radical molecule thiol end-capped penta phenylene ethynylene (OPE5). By controlling the relative position of the introduced electrons in the free radical molecules, ferromagnetic or antiferromagnetic coupling can be formed, so as to control the spin state of free radical molecules.[91]

When the spin is related to electron transport, selection rules need to be considered, which results in some subtle characteristics of the transport properties.[93] For example, molecules with a high-spin state can appear the ground state spin blockade (Fig. 8e).[94] It is not enough to clarify the resistance change during the transport process through the *I–V* test of the two-terminal single magnetic molecule devices. It is very necessary to systematically study the electron transport in the single magnetic molecule FET. For example, Yoshida *et al.* studied the tunnelling magnetoresistance (TMR) of single C_{60} molecule FETs with nickel electrodes. In the entire test bias, the tunnel magnetoresistance can be adjusted by the gate voltage of up to −80%. The TMR is always negative in the range, which is caused by the new hybrid state generated at the interface between the nickel electrode and the C_{60} molecule (Fig. 8f).[39] Therefore, as mentioned above, single-molecule FETs play an important role in modulating spin states and exploring spin transport of single molecules.

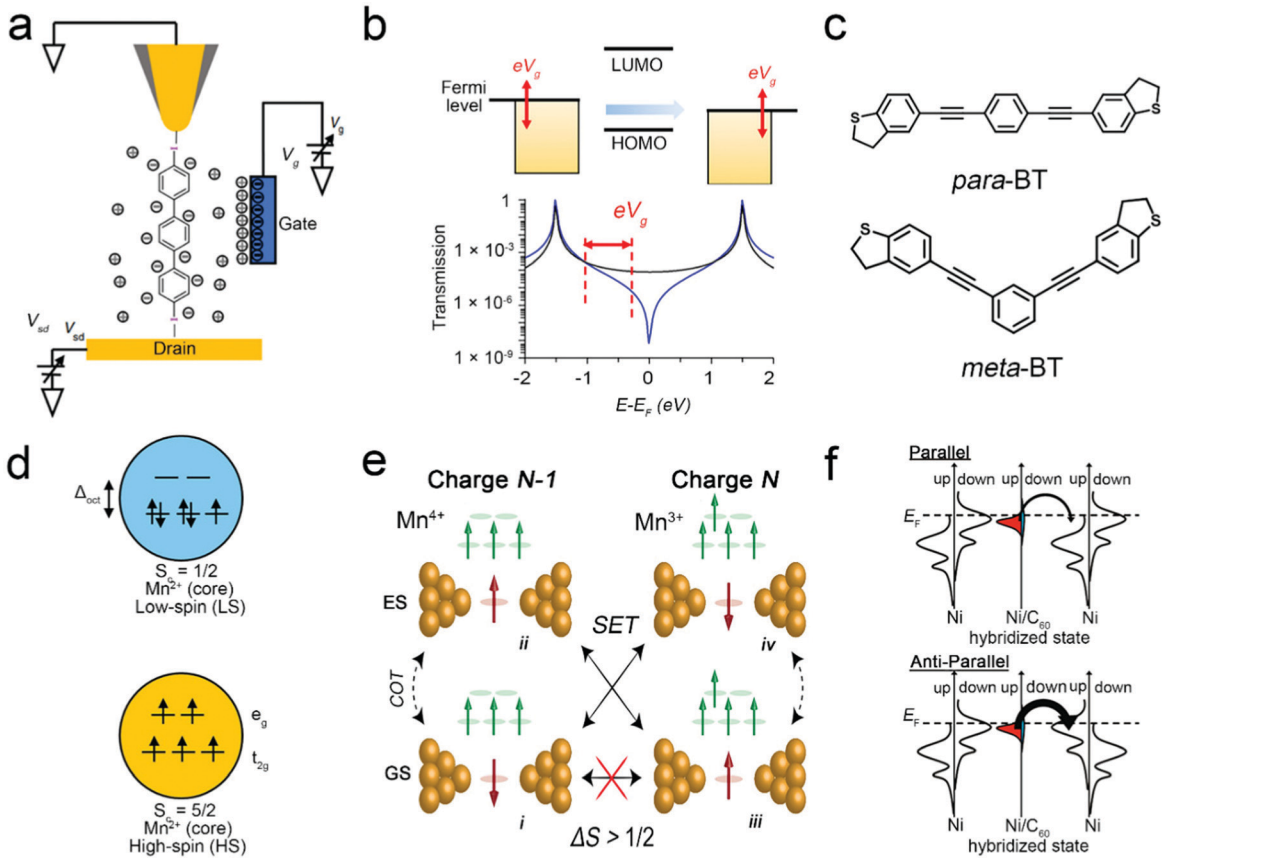

Fig. 8 (a) Schematic view of the gate-controlled measurement of single-molecule junctions. (b) Top: Adjusting the gate voltage changes the arrangement of molecular levels relative to the Fermi levels. Bottom: Representative transfer functions for constructive (black) and destructive (blue) interference cases.[87] Copyright: 2019, Springer Nature Limited. (c) Chemical structures of the molecules *para*-BT and *meta*-BT.[86] Copyright: 2018, American Chemical Society. (d) Two different d^5 electronic configurations of the Mn^{2+} nuclear spin crossing.[23] Copyright: 2010, American Chemical Society. (e) Diagram showing the four states of different charge and spin, where the red and green arrows correspond to the ligand spin and the spins in the Mn center, respectively.[92] Copyright: 2019, American Physical Society. (f) Schematic representation of spin-resolved density of states and spin-dependent electron tunnelling in a Ni/C_{60}/Ni junction when the two Ni electrodes are in the parallel magnetization configuration (upper) and the antiparallel magnetization configuration (lower).[39] Copyright: 2013, American Chemical Society.

4.3 Regulation of the thermoelectric effect

The thermoelectric effect describes the interaction between heat and charge flow. Single-molecule FETs are an ideal platform for exploring the thermoelectric effects at the single-molecule level. Specifically, the thermoelectric efficiency is expressed by the dimensionless quality factor $ZT = (GS^2/\kappa)T$, where T represents the average temperature, G represents the conductance and κ represents the sum of the contributions of electrons and phonons to the thermal conductance. In traditional thermoelectric materials, S, G, and κ are mutually restricted, which is not conducive to the improvement of thermoelectric efficiency, while in single-molecule devices, they can be improved at the same time. For instance, Kim *et al.* introduced a temperature difference in a single-molecule FET to achieve electrostatically controlled thermoelectric properties, which is confirmed in the test of Au–biphenyl-4,4′-dithiol–Au and Au–fullerene–Au single-molecule FETs, as shown in Fig. 9a and b. The Seebeck coefficient and conductance can be simultaneously increased by electrostatic control (Fig. 9c). This improvement in thermoelectric performance is essentially due to the fact that the main transmission channel of molecules is brought closer to the Fermi level of the electrode through electrostatic control.[95] Gehring *et al.* also achieved electrostatically controlled thermoelectric properties in a fullerene single-molecule FET composed of graphene electrodes. By replacing metal electrodes with graphene electrodes, the shielding effect on the gate is reduced. The adjustment range of the main molecular transmission orbital is further improved, and the energy factor GS^2 is close to the theoretical limit of the isolated Breit–Wigner resonance.[96] Therefore, by adjusting the main transmission orbital by electrostatic control to approach the Fermi level, the thermoelectric performance of the single-molecular FET can be effectively improved.

4.4 Regulation of superconductivity

When superconducting electrodes are used for constructing single-molecule FETs, interesting physical phenomena can be observed. For instance, for the single-molecule devices with magnetic molecules, the Cooper pair will compete with the Kondo shield, causing the Cooper pair to be broken and produce a Shiba state.[97] Single C_{60} molecules are connected

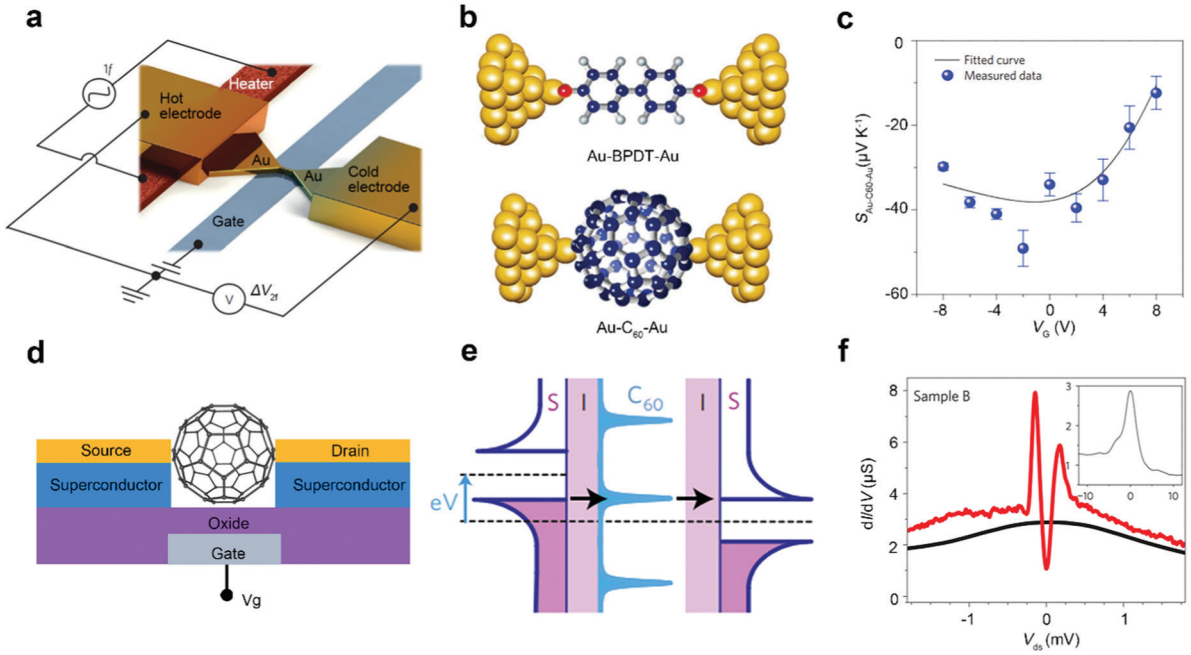

Fig. 9 (a) Schematic of the electromigrated break junction with an integrated heater. (b) Schematic diagram of the structure of single-molecule junctions with BPDT and C_{60} molecules. (c) The Seebeck coefficient diagram of an Au–C_{60}–Au single-molecule junction.[95] Copyright: 2014, Macmillan Publishers Limited. (d) Schematic of C_{60} single-molecule FETs constructed with superconductor electrodes. (e) Schematic of the corresponding energy level alignment for minimal bias voltage conditions allowing for the finite current flow. (f) d*I*/d*V* as a function of drain–source voltage (V_{ds}) at a constant gate voltage ($T < 40$ mK) and in both the normal (black line) and the superconducting state (red line). The inset shows the normal-state data over a larger bias-voltage window.[40] Copyright: 2009, Macmillan Publishers Limited.

to aluminum electrodes to achieve superconductivity in single-molecule FETs (Fig. 9d and e). It is found that when the coupling strength between the molecule and the electrode changes in a wide range, the Coulomb blockade effect, Kondo effect and the superconductivity show a coexistence and competition relationship (Fig. 9f).[40] Furthermore, when the ring-shaped molecule is connected to the superconducting electrodes, a single-molecule superconducting FET can be constructed. Specifically, a single-molecule superconducting FET model is theoretically constructed with a benzene ring as a prototype. When quantum interference occurs, the Cooper pair can transport through the molecule. Therefore, superconductivity can be achieved by the gated control of quantum interference.[82]

5. Summary and outlook

In summary, a single-molecule FET is one kind of key electronic device with both important basic research and future application value. Single-molecule FETs can be used as an important platform for studying the physical and chemical mechanisms at the single-molecule level. Therefore, single-molecule FETs with different structures are designed for different applications. At present, single-molecule devices based on liquid or solid gates have been developed. For liquid gate systems with electrolyte solutions or ionic liquids, when a gate voltage is applied, an electric double layer is formed around the molecules, thereby applying a gate electric field to a single molecule. Since the thickness of the electric double layer is determined by the size of the used ions, a large gate electric field can be applied to achieve a strong gate control capability. Solid-state gates can better meet the basic conditions of some practical applications, such as exploring the physical mechanism of single molecules at low temperatures. However, the current development of single-molecule devices with solid-state gates still faces many challenges, such as how to construct high-performance dielectric layers at the molecular scale.

The essential mechanism of the single-molecule FET is to change the potential energy of the molecule by applying a gate electric field, thereby changing the relative position between the molecular orbital and the Fermi level. The interface coupling between the molecule and the electrode has a great influence on the performance of the single-molecule FET. When the coupling strength is different, the single-molecule FET will show different characteristics. In the case of weak coupling, electron transfer in a single-molecule FET is a two-step process, and Coulomb blockade occurs; in the case of strong coupling, the electron transfer becomes a one-step coherent process. The uniquely designed single-molecule FETs can also be used to adjust quantum interference, spin and thermoelectric and superconducting properties. For instance, based on the field effect mechanism of single-molecule devices, quantum interference can be effectively adjusted to improve the switching ratio of the devices, the spin state of the molecules can be controlled to explore the spin transport characteristics, and the thermoelectric effect of single molecules can be regulated to improve the thermoelectric conversion efficiency.

Despite such tremendous progress, to realize the iterative development of single-molecule FETs, new architectures and new systems need to be developed. It is also necessary to introduce new research methods, such as ultra-low temperature, strong magnetic field, femtosecond laser, and terahertz, to reveal the physical mechanism. The application of single-molecule FETs should not only be expanded on the existing basis, but also give full play to the advantages of single molecules as quantum systems. In addition, for the future development of integrated circuits based on single-molecule devices, the highly successful fabrication and integration of solid-state gated devices will invite intense research.

Author contributions

X. F. G., C. C. J. and H. Y. F. conceived the main concept of the review article. H. Y. F. and X. Z. collected the related information needed in writing the paper. H. Y. F., X. Z., P. H. L., M. M. L., L. Y., C. C. J. and X. F. G. wrote and modified the manuscript. All authors discussed and commented on the manuscript.

Conflicts of interest

There are no conflicts to declare.

Acknowledgements

We are grateful to the National Key R&D Program of China (2017YFA0204901), the NSFC (21727806, 21933001 and 22173050), the NSFB (Z181100004418003), the Frontiers Science Center for New Organic Matter at Nankai University (63181206) and the Tencent Foundation through the EXPLORER PRIZE for their financial support of this work.

Notes and references

1 H. Park, J. Park, A. K. L. L. Lim, E. H. Anderson, A. P. Alivisatos and P. L. McEuen, *Nature*, 2000, **407**, 57–60.
2 X. Guo, J. P. Small, J. E. Klare, Y. W. Wang, M. S. Purewal, I. W. Tam, B. H. Hong, R. Caldwell, L. Huang, S. O'Brien, J. Yan, R. Breslow, S. J. Wind, J. Hone, P. Kim and C. Nuckolls, *Science*, 2006, **311**, 356–359.
3 B. Chen and K. Xu, *NANO*, 2019, **14**, 1930007.
4 W. Zhao, D. Zou, Z. Sun, Y. Xu, G. Ji, X. Li and C. Yang, *Adv. Theory Simul.*, 2020, **3**, 2000163.
5 J. Bai, X. Li, Z. Zhu, Y. Zheng and W. Hong, *Adv. Mater.*, 2021, 2005883.
6 M. L. Perrin, E. Burzuri and H. S. van der Zant, *Chem. Soc. Rev.*, 2015, **44**, 902–919.
7 P. Li, C. Jia and X. Guo, *Chem. Rec.*, 2021, **21**, 1284–1299.
8 N. Roch, S. Florens, V. Bouchiat, W. Wernsdorfer and F. Balestro, *Nature*, 2008, **453**, 633–637.
9 J. Hwang, M. Pototschnig, R. Lettow, G. Zumofen, A. Renn, S. Gotzinger and V. Sandoghdar, *Nature*, 2009, **460**, 76–80.
10 S. Sorgenfrei, C. Y. Chiu, R. L. Gonzalez, Jr., Y. J. Yu, P. Kim, C. Nuckolls and K. L. Shepard, *Nat. Nanotechnol.*, 2011, **6**, 126–132.
11 S. Richter, E. Mentovich and R. Elnathan, *Adv. Mater.*, 2018, **30**, 1706941.
12 A. R. Champagne, A. N. Pasupathy and D. C. Ralph, *Nano Lett.*, 2005, **5**, 305–308.
13 N. J. Kay, S. J. Higgins, J. O. Jeppesen, E. Leary, J. Lycoops, J. Ulstrup and R. J. Nichols, *J. Am. Chem. Soc.*, 2012, **134**, 16817–16826.
14 D. Xiang, H. Jeong, D. Kim, T. Lee, Y. Cheng, Q. Wang and D. Mayer, *Nano Lett.*, 2013, **13**, 2809–2813.
15 S. Cardona-Serra and A. Gaita-Arino, *Dalton Trans.*, 2018, **47**, 5533–5537.
16 C. Wu, X. Qiao, C. M. Robertson, S. J. Higgins, C. Cai, R. J. Nichols and A. Vezzoli, *Angew. Chem., Int. Ed.*, 2020, **59**, 12029–12034.
17 Y. H. Wang, F. Yan, D. F. Li, Y. F. Xi, R. Cao, J. F. Zheng, Y. Shao, S. Jin, J. Z. Chen and X. S. Zhou, *J. Phys. Chem. Lett.*, 2021, **12**, 758–763.
18 P. Li, C. Jia and X. Guo, *Chin. J. Chem.*, 2021, **39**, 223–231.
19 N. Xin, X. Kong, Y. P. Zhang, C. Jia, L. Liu, Y. Gong, W. Zhang, S. Wang, G. Zhang, H. L. Zhang, H. Guo and X. Guo, *Adv. Electron. Mater.*, 2020, **6**, 1901237.
20 K. Moth-Poulsen and T. Bjornholm, *Nat. Nanotechnol.*, 2009, **4**, 551–556.
21 H. Yu, Y. Luo, K. Beverly, J. F. Stoddart, H.-R. Tseng and J. R. Heath, *Angew. Chem.*, 2003, **115**, 5884–5889.
22 H. Song, Y. Kim, Y. H. Jang, H. Jeong, M. A. Reed and T. Lee, *Nature*, 2009, **462**, 1039–1043.
23 E. A. Osorio, K. Moth-Poulsen, H. S. van der Zant, J. Paaske, P. Hedegard, K. Flensberg, J. Bendix and T. Bjornholm, *Nano Lett.*, 2010, **10**, 105–110.
24 W. Liang, M. P. Shores, M. Bockrath, J. R. Long and H. Park, *Nature*, 2002, **417**, 725–729.
25 L. H. Yu, Z. K. Keane, J. W. Ciszek, L. Cheng, M. P. Stewart, J. M. Tour and D. Natelson, *Phys. Rev. Lett.*, 2004, **93**, 266802.
26 A. D. Shkop, O. M. Bahrova, S. I. Kulinich and I. V. Krive, *Superlattice. Microst.*, 2020, **137**, 106356.
27 K. Yoshida, K. Shibata and K. Hirakawa, *Phys. Rev. Lett.*, 2015, **115**, 138302.
28 C. S. Lau, H. Sadeghi, G. Rogers, S. Sangtarash, P. Dallas, K. Porfyrakis, J. Warner, C. J. Lambert, G. A. Briggs and J. A. Mol, *Nano Lett.*, 2016, **16**, 170–176.
29 Y. Li, J. A. Mol, S. C. Benjamin and G. A. Briggs, *Sci. Rep.*, 2016, **6**, 33686.
30 Z. Zhang, F. Yin, C. Wang, Z. Li and H. Liu, *J. Phys.: Condens. Matter*, 2021, **33**, 235302.
31 A. W. Ghosh, T. Rakshit and S. Datta, *Nano Lett.*, 2004, **4**, 565–568.
32 F. Jackel, M. D. Watson, K. Mullen and J. P. Rabe, *Phys. Rev. Lett.*, 2004, **92**, 188303.
33 C. Jia, Z. Lin, Y. Huang and X. Duan, *Chem. Rev.*, 2019, **119**, 9074–9135.
34 P. Wang, C. Jia, Y. Huang and X. Duan, *Matter*, 2021, **4**, 552–581.

35 J. Gao, Y. Zheng, W. Yu, Y. Wang, T. Jin, X. Pan, K. P. Loh and W. Chen, *SmartMat.*, 2021, **2**, 88–98.
36 A. Cui, H. Dong and W. Hu, *Small*, 2015, **11**, 6115–6141.
37 Y. Kim, C. H. Ang, K. Ang and S. W. Chang, *J. Vac. Sci. Technol., B*, 2021, **39**, 010802.
38 J. Park, A. N. Pasupathy, J. I. Goldsmith, C. Chang, Y. Yaish, J. R. Petta, M. Rinkoski, J. P. Sethna, H. D. Abruna, P. L. McEuen and D. C. Ralph, *Nature*, 2002, **417**, 722–725.
39 K. Yoshida, I. Hamada, S. Sakata, A. Umeno, M. Tsukada and K. Hirakawa, *Nano Lett.*, 2013, **13**, 481–485.
40 C. B. Winkelmann, N. Roch, W. Wernsdorfer, V. Bouchiat and F. Balestro, *Nat. Phys.*, 2009, **5**, 876–879.
41 M. A. Reed, C. Zhou, C. J. Muller, T. P. Burgin and J. M. Tour, *Science*, 1997, **278**, 252–254.
42 C. A. Martin, J. M. van Ruitenbeek and H. S. van der Zant, *Nanotechnology*, 2010, **21**, 265201.
43 S. Ballmann and H. B. Weber, *New J. Phys.*, 2012, **14**, 123028.
44 C. Jia, B. Ma, N. Xin and X. Guo, *Acc. Chem. Res.*, 2015, **48**, 2565–2575.
45 M. Sun, C. Zhang, D. Chen, J. Wang, Y. Ji, N. Liang, H. Gao, S. Cheng and H. Liu, *SmartMat.*, 2021, **2**, 213–225.
46 A. Bergvall, K. Berland, P. Hyldgaard, S. Kubatkin and T. Löfwander, *Phys. Rev. B: Condens. Matter Mater. Phys.*, 2011, **84**, 155451.
47 F. Prins, A. Barreiro, J. W. Ruitenberg, J. S. Seldenthuis, N. Aliaga-Alcalde, L. M. Vandersypen and H. S. van der Zant, *Nano Lett.*, 2011, **11**, 4607–4611.
48 Y. Cao, S. Dong, S. Liu, Z. Liu and X. Guo, *Angew. Chem., Int. Ed.*, 2013, **52**, 3906–3910.
49 J. A. Mol, C. S. Lau, W. J. Lewis, H. Sadeghi, C. Roche, A. Cnossen, J. H. Warner, C. J. Lambert, H. L. Anderson and G. A. Briggs, *Nanoscale*, 2015, **7**, 13181–13185.
50 H. Sun, X. Liu, Y. Su, B. Deng, H. Peng, S. Decurtins, S. Sanvito, S. X. Liu, S. Hou and J. Liao, *Nanoscale*, 2019, **11**, 13117–13125.
51 C. Huang, A. V. Rudnev, W. Hong and T. Wandlowski, *Chem. Soc. Rev.*, 2015, **44**, 889–8901.
52 R. J. Nichols and S. J. Higgins, *Acc. Chem. Res.*, 2016, **49**, 2640–2648.
53 B. Xu, X. Xiao, X. Yang, L. Zang and N. Tao, *J. Am. Chem. Soc.*, 2005, **127**, 2386–2387.
54 R. J. Brooke, C. Jin, D. S. Szumski, R. J. Nichols, B. W. Mao, K. S. Thygesen and W. Schwarzacher, *Nano Lett.*, 2015, **15**, 275–280.
55 N. Xin, X. Li, C. Jia, Y. Gong, M. Li, S. Wang, G. Zhang, J. Yang and X. Guo, *Angew. Chem., Int. Ed.*, 2018, **57**, 14026–14031.
56 M. Famili, C. Jia, X. Liu, P. Wang, I. M. Grace, J. Guo, Y. Liu, Z. Feng, Y. Wang, Z. Zhao, S. Decurtins, R. Häner, Y. Huang, S.-X. Liu, C. J. Lambert and X. Duan, *Chem*, 2019, **5**, 474–484.
57 C. Jia, I. M. Grace, P. Wang, A. Almeshal, Z. Huang, Y. Wang, P. Chen, L. Wang, J. Zhou, Z. Feng, Z. Zhao, Y. Huang, C. J. Lambert and X. Duan, *Chem*, 2020, **6**, 1172–1182.
58 C. Jia, M. Famili, M. Carlotti, Y. Liu, P. Wang, I. M. Grace, Z. Feng, Y. Wang, Z. Zhao, M. Ding, X. Xu, C. Wang, S.-J. Lee, Y. Huang, R. C. Chiechi, C. J. Lambert and X. Duan, *Sci. Adv.*, 2018, **4**, eaat8237.
59 L. Li, W. Y. Lo, Z. Cai, N. Zhang and L. Yu, *Chem. Sci.*, 2016, **7**, 3137–3141.
60 N. Zhang, W. Y. Lo, Z. Cai, L. Li and L. Yu, *Nano Lett.*, 2017, **17**, 308–312.
61 C. Jia, A. Migliore, N. Xin, S. Huang, J. Wang, Q. Yang, S. Wang, H. Chen, D. Wang, B. Feng, Z. Liu, G. Zhang, D. Qu, H. Tian, M. A. Ratner, H. Q. Xu, A. Nitzan and X. Guo, *Science*, 2016, **352**, 1443–1445.
62 C. Jia, J. Wang, C. Yao, Y. Cao, Y. Zhong, Z. Liu, Z. Liu and X. Guo, *Angew. Chem., Int. Ed.*, 2013, **52**, 8666–8670.
63 A. C. Whalley, M. L. Steigerwald, X. Guo and C. Nuckolls, *J. Am. Chem. Soc.*, 2007, **129**, 12590–12591.
64 L. Meng, N. Xin, C. Hu, J. Wang, B. Gui, J. Shi, C. Wang, C. Shen, G. Zhang, H. Guo, S. Meng and X. Guo, *Nat. Commun.*, 2019, **10**, 1450.
65 M. L. Perrin, C. J. Verzijl, C. A. Martin, A. J. Shaikh, R. Eelkema, J. H. van Esch, J. M. van Ruitenbeek, J. M. Thijssen, H. S. van der Zant and D. Dulic, *Nat. Nanotechnol.*, 2013, **8**, 282–287.
66 Z. Li, H. Li, S. Chen, T. Froehlich, C. Yi, C. Schonenberger, M. Calame, S. Decurtins, S. X. Liu and E. Borguet, *J. Am. Chem. Soc.*, 2014, **136**, 8867–8870.
67 B. Limburg, J. O. Thomas, G. Holloway, H. Sadeghi, S. Sangtarash, I. C.-Y. Hou, J. Cremers, A. Narita, K. Müllen, C. J. Lambert, G. A. D. Briggs, J. A. Mol and H. L. Anderson, *Adv. Funct. Mater.*, 2018, **28**, 1803629.
68 B. Capozzi, Q. Chen, P. Darancet, M. Kotiuga, M. Buzzeo, J. B. Neaton, C. Nuckolls and L. Venkataraman, *Nano Lett.*, 2014, **14**, 1400–1404.
69 I. D. E. Prez, Z. Li, S. Guo, C. Madden, H. Huang, Y. Che, X. Yang, L. Zang and N. Tao, *ACS Nano*, 2012, **6**, 7044–7052.
70 A. Xiang, H. Li, S. Chen, S. X. Liu, S. Decurtins, M. Bai, S. Hou and J. Liao, *Nanoscale*, 2015, **7**, 7665–7673.
71 S. Kubatkin, A. Danilov, M. Hjort, J. R. M. Cornil, J.-L. B. Das, N. Stuhr-Hansen, P. H. Rd and T. Bjørnholm, *Nature*, 2003, **425**, 698–701.
72 D. Goldhaber-Gordon, H. Shtrikman, D. Mahalu, D. Abusch-Magder, U. Meirav and M. A. Kastner, *Nature*, 1998, **391**, 156–159.
73 L. H. Yu, Z. K. Keane, J. W. Ciszek, L. Cheng, J. M. Tour, T. Baruah, M. R. Pederson and D. Natelson, *Phys. Rev. Lett.*, 2005, **95**, 256803.
74 E. A. Osorio, K. O'Neill, M. Wegewijs, N. Stuhr-Hansen, J. Paaske, T. Bjørnholm and H. S. J. van der Zant, *Nano Lett.*, 2007, **7**, 3336–3342.
75 G. D. Scott and D. Natelson, *ACS Nano*, 2010, **4**, 3560–3579.
76 Z.-Z. Chen, R. Lü and B.-F. Zhu, *Phys. Rev. B: Condens. Matter Mater. Phys.*, 2005, **71**, 165324.
77 S. Du, K. Yoshida, Y. Zhang, I. Hamada and K. Hirakawa, *Nat. Photonics*, 2018, **12**, 608–612.
78 E. Burzuri, Y. Yamamoto, M. Warnock, X. Zhong, K. Park, A. Cornia and H. S. van der Zant, *Nano Lett.*, 2014, **14**, 3191–3196.
79 P. Gehring, J. M. Thijssen and H. S. J. van der Zant, *Nat. Rev. Phys.*, 2019, **1**, 381–396.

80 K. Joulain, J. Drevillon, Y. Ezzahri and J. Ordonez-Miranda, *Phys. Rev. Lett.*, 2016, **116**, 200601.
81 R. Miao, H. Xu, M. Skripnik, L. Cui, K. Wang, K. G. L. Pedersen, M. Leijnse, F. Pauly, K. Warnmark, E. Meyhofer, P. Reddy and H. Linke, *Nano Lett.*, 2018, **18**, 5666–5672.
82 C. Nappi, F. Romeo, L. Parlato, F. Di Capua, A. Aloisio and E. Sarnelli, *J. Phys. Chem. C*, 2018, **122**, 11498–11504.
83 Y. Li, L. Zhao, Y. Yao and X. Guo, *ACS Appl. Bio Mater.*, 2019, **3**, 68–85.
84 Y. Li, C. Yang and X. Guo, *Acc. Chem. Res.*, 2020, **53**, 159–169.
85 N. Darwish, I. Diez-Perez, P. Da Silva, N. Tao, J. J. Gooding and M. N. Paddon-Row, *Angew. Chem.*, 2012, **51**, 3257–3260.
86 X. Liu and S. Sangtarash, *Angew. Chem., Int. Ed.*, 2017, **56**, 173–176.
87 M. Koole, J. M. Thijssen, H. Valkenier, J. C. Hummelen and H. S. van der Zant, *Nano Lett.*, 2015, **15**, 5569–5573.
88 B. Huang, X. Liu, Y. Yuan, Z. W. Hong, J. F. Zheng, L. Q. Pei, Y. Shao, J. F. Li, X. S. Zhou, J. Z. Chen, S. Jin and B. W. Mao, *J. Am. Chem. Soc.*, 2018, **140**, 17685–17690.
89 Y. Li, M. Buerkle, G. Li, A. Rostamian, H. Wang, Z. Wang, D. R. Bowler, T. Miyazaki, L. Xiang, Y. Asai, G. Zhou and N. Tao, *Nat. Mater.*, 2019, **18**, 357–363.
90 J. Bai, A. Daaoub, S. Sangtarash, X. Li, Y. Tang, Q. Zou, H. Sadeghi, S. Liu, X. Huang, Z. Tan, J. Liu, Y. Yang, J. Shi, G. Meszaros, W. Chen, C. Lambert and W. Hong, *Nat. Mater.*, 2019, **18**, 364–369.
91 J. Fock, M. Leijnse, K. Jennum, A. S. Zyazin, J. Paaske, P. Hedegård, M. Brøndsted Nielsen and H. S. J. van der Zant, *Phys. Rev. B: Condens. Matter Mater. Phys.*, 2012, **86**, 235403.
92 S. Thiele, R. Vincent, M. Holzmann, S. Klyatskaya, M. Ruben, F. Balestro and W. Wernsdorfer, *Phys. Rev. Lett.*, 2013, **111**, 037203.
93 F. Troiani, C. Godfrin, S. Thiele, F. Balestro, W. Wernsdorfer, S. Klyatskaya, M. Ruben and M. Affronte, *Phys. Rev. Lett.*, 2017, **118**, 257701.
94 J. de Bruijckere, P. Gehring, M. Palacios-Corella, M. Clemente-Leon, E. Coronado, J. Paaske, P. Hedegard and H. S. J. van der Zant, *Phys. Rev. Lett.*, 2019, **122**, 197701.
95 Y. Kim, W. Jeong, K. Kim, W. Lee and P. Reddy, *Nat. Nanotechnol.*, 2014, **9**, 881–885.
96 P. Gehring, A. Harzheim, J. Spiece, Y. Sheng, G. Rogers, C. Evangeli, A. Mishra, B. J. Robinson, K. Porfyrakis, J. H. Warner, O. V. Kolosov, G. A. D. Briggs and J. A. Mol, *Nano Lett.*, 2017, **17**, 7055–7061.
97 J. O. Island, R. Gaudenzi, J. de Bruijckere, E. Burzuri, C. Franco, M. Mas-Torrent, C. Rovira, J. Veciana, T. M. Klapwijk, R. Aguado and H. S. van der Zant, *Phys. Rev. Lett.*, 2017, **118**, 117001.